Published in IET Microwaves, Antennas & Propagation
Received on 29th December 2008
Revised on 30th August 2009
doi: 10.1049/iet-map.2008.0444

ISSN 1751-8725

Design of a small antenna for wideband mobile direction finding systems

C. Cho[1] *I. Park*[2] *H. Choo*[3]

[1]*Institute of Advanced Technologies, Samsung Thales, Yongin, Korea*
[2]*Department of Electrical and Computer Engineering, Ajou University, Suwon, Korea*
[3]*School of Electronic and Electrical Engineering, Hongik University, Seoul, Korea*
E-mail: hschoo@hongik.ac.kr

Abstract: In this study, the authors propose a novel small antenna for use in mobile direction finding (DF) systems covering the range 20–1300 MHz. The proposed antenna has a multiconical sleeve to increase the input resistance at low frequencies while reducing the antenna size. A skirt-shaped disk on top of the antenna body maintains the omnidirectional radiation pattern over a wide frequency band without radiation nulls in the broadside direction. The detailed design parameters of the proposed antenna were optimised using a Pareto genetic algorithm (GA) with the FEKO EM software package. Below 200 MHz, the proposed antenna shows a receiving performance comparable to a 60-cm conventional dipole but at only half the size. Above 200 MHz, the antenna maintains an omnidirectional radiation pattern up to 1300 MHz with a stable realised gain, whereas the 60-cm dipole has a broadside radiation null at about 850 MHz.

1 Introduction

Mobile direction finding (DF) systems are used in many applications for estimating the direction of unknown electromagnetic waves. Mobile DF systems have been frequently used in the military to detect enemy locations by their radio-frequency communications. Mobile DF systems are also currently used for various non-military applications such as detecting unauthorised transmitters, finding shadow zones of various wireless services and for ground-penetrating radars [1–7].

Most DF systems determine the direction of electromagnetic waves by calculating the phase differences of an array of antennas. Ideally, each antenna in the array has an omnidirectional radiation pattern to maintain uniform receiving characteristics that are independent of the direction of the arriving signals. Generally, antennas with a symmetrical structure in the azimuth plane such as a simple dipole, a biconical antenna or a loaded disk dipole exhibit omnidirectional radiation patterns. These antennas, however, cannot be used over a wide frequency band since radiation nulls are present in the broadside direction ($\theta = 90^{\circ}$) when induced currents in the antenna body are distributed on an even number of wavelengths [8–11].

The disk-loaded monopole with inserted positive-intrinsic-negative (PIN) diodes has been used to provide a mobile DF antenna with broadband characteristics and increased usable frequency range by controlling induced currents on the antenna body. However, the added PIN diodes and the accompanying bias networks increase the complexity and manufacturing cost of the system [12, 13]. A low radar cross-section (RCS) antenna with an improved receiving antenna performance has been reported, but the complicated antenna structure required to minimise the RCS is not suitable for a mobile DF system [14].

In this paper, we propose a novel small antenna with a compact structure as an element of a mobile DF system for finding the direction of electromagnetic waves in the range 20–1300 MHz. In the low-frequency region (20–200 MHz), the proposed antenna uses a multiconical sleeve to provide an input resistance comparable to a 60-cm dipole at half the physical size. In the high-frequency region (200–1300 MHz), the proposed antenna achieves a wideband omnidirectional radiation pattern without nulls in the broadside direction by using a skirt-shaped disk on top of the antenna body. This behaviour is unlike that of the 60-cm dipole, which has a broadside radiation null at about 850 MHz.

This paper is organised as follows. Section 2 presents the geometry of the proposed small mobile DF antenna and the details of implementing the genetic algorithm (GA). Section 3 describes the measurement results and the operating principles of the antenna and Section 4 gives the conclusions.

2 Design procedure using a Pareto GA

The objective of this study was to design a small antenna for integration into a vehicle-mounted DF array system operating over a wide frequency band. To be suitable for the mobile DF system, each antenna should have appropriate receiving characteristics from the shortwave to the ultra-high-frequency (UHF) band (20–1300 MHz). The height of the antenna is restricted to 30 cm for easy installation on the vehicle, and the diameter is restricted to 10 cm to maintain the phase difference among the neighbouring antennas to less than 180° [15, 16]. A low noise amplifier (LNA) is usually installed at the input of the DF antenna to detect extremely weak signals since the DF system may be located far away from the source of the unknown electromagnetic waves. A conventional LNA generally increases the antenna gain by about 15 dB and the detection sensitivity for the signal is about −80 dBm. Thus, the gain of the DF antenna should be greater than −15 dBi to detect 1-W signals at a distance of 10 km. Below frequencies of 200 MHz, however, it is extremely difficult for antennas to maintain a realised gain greater than −15 dBi since the electrical size of the antenna is very small compared to the wavelength, and the input resistance of the antenna is less than a few ohms. In that case, the received signal power is maximally transferred to the LNA when the antenna is designed to have the highest input resistance possible instead of matching the nominal 50-Ω characteristic impedance. Above 200 MHz, the antenna should have an omnidirectional radiation pattern over a wide bandwidth without broadside nulls to achieve stable performance. In addition, the antenna should maintain a broad beamwidth greater than 90° with a gain greater than −15 dBi to receive any signal arriving off the bore-sight angle without requiring an electrical or mechanical beam-steering system.

To satisfy the above specifications, we propose a new small-profile DF antenna as shown in Fig. 1. We inserted a multiconical sleeve in the antenna structure to increase the input resistance in the low-frequency region (20–200 MHz). We also added a disk load to the top of the antenna body to achieve an omnidirectional radiation pattern over a wide bandwidth without nulls in the broadside direction. The disk loading has the effect of shifting the frequency where the radiation null occurs to a much higher frequency while the other characteristics remain almost the same as before. The edge of the loaded disk is bent down to form a skirt shape to maximise the disk loading effect since the diameter of the antenna is restricted to less than 10 cm. Finally, we use an aluminium cylinder with a radius of 8 mm as the antenna body to support the heavy disk and the multiconical sleeve even under strong wind conditions.

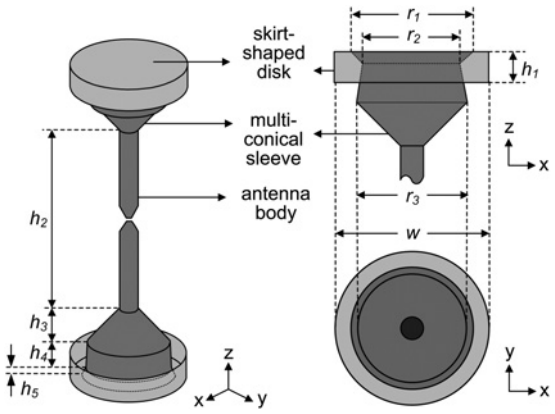

Figure 1 *Geometry of the proposed small DF antenna*

Two design goals were sought in the creation of this antenna. One was to raise the input resistance to be comparable to that of the 60-cm dipole while keeping the antenna size under 30 cm in the low-frequency band. The other was to maintain the omnidirectional radiation pattern up to 1300 MHz with a high realised gain.

We used a Pareto GA in conjunction with the FEKO software package (EM Software and Systems) [17] to determine the optimal design parameters. The GA is a stochastic search method based on the principles of natural selection and evolution, and it has been applied to many EM design problems. The Pareto GA in particular produces good results for multi-objective problems because it can generate a wide range of solutions corresponding to more than one objective with only one optimisation cycle [18–20]. In addition, FEKO provides highly accurate results for a three-dimensional (3D) structure such as the proposed antenna with a relatively fast calculation time compared to other EM simulation tools with different solvers. In the Pareto GA process, a two-dimensional (2D) cross-section of the antenna shape is encoded as a 90-bit binary chromosome, and in the process of EM simulation, the encoded 2D shape is rotated around the z-axis to form a complete 3D antenna structure for proper EM simulation. The EM simulation time can be reduced to approximately two-third if the 3D axial symmetric structure is properly modelled as a 2D structure by using the electric and magnetic boundary conditions. In the Pareto GA processes, evolution of the optimisation is determined by the cost function, which explicitly expresses the design goals as a formula. The cost functions used in this Pareto GA process are as follows

$$\text{cost}\,1 = 1 - \sum_{i=1}^{n} \frac{R_{\text{ant}}(f_i) \times \text{Eff}_{\text{ant}}}{R_{\text{dipole}}(f_i)} \quad (20\,\text{MHz} < f_i < 200\,\text{MHz}) \tag{1}$$

$$\text{cost}\,2 = 1 - \frac{\sum_{i=1}^{n}\sum_{j=1}^{m} \text{Gain}(f_i, \theta_j)}{m \times n} \quad (200\,\text{MHz} < f_i < 1300\,\text{MHz},\ \pi/6 < \theta_j < 5\pi/6) \tag{2}$$

where R_{ant} and R_{dipole} are the input resistances of the proposed antenna and the conventional 60-cm dipole, respectively, and Eff_{ant} is the radiation efficiency of the proposed antenna. Cost 1 is used for high-input resistance in the low-frequency band and is normalised by the input resistance of the conventional 60-cm dipole. For example, the conventional 60-cm dipole has an input resistance of 0.25–45.5 Ω from 20 to 200 MHz, and the input resistances of the optimised antennas are divided by those values at each frequency. Cost 2 is used to raise the antenna gain and broaden the beamwidth, and is calculated by subtracting the averaged gain from 1, where the observation angle is $\pi/6 < \theta < 5\pi/6$. The m and n represent the number of discrete observation angles and frequencies within the frequency and angle range of interest. The Pareto GA then minimises both Cost 1 and Cost 2 to find solutions. After evaluating all populations (one population consists of 50 chromosomes) by the above two cost functions using the FEKO EM simulator, each chromosome is ranked using the non-dominating ranking method [21]. Then the population for the next generation is reproduced using a two-point crossover scheme with a mutation probability of 0.1 and a crossover probability of 0.8. Additionally, a sharing scheme is applied to each sample to obtain a widely spread result in terms of the two cost domains [22]. Roughly 200 GA iterations with 50 chromosomes were required to obtain converged results. This required less than 120 h using four Intel Q6600 CPUs. If the EM simulation time for each design were much longer than this situation, a local optimiser or hybrid method should be considered instead of GA for faster convergence [23, 24]. The Pareto GA optimised result is shown in Fig. 2, where the average gain in the high-frequency band (200–1300 MHz) is plotted against the normalised radiation resistance in the low-frequency band (20–200 MHz). As expected, the radiation resistance in the low-frequency band increased when the average gain in the high-frequency band decreased. All the optimised samples achieved average antenna gains greater than −6 dBi and normalised radiation resistances greater than 0.75 Ω, whereas the 60-cm dipole exhibited an average gain of −10 dB and a radiation resistance of approximately 1 Ω. At a low-frequency band (20–200 MHz), the performance of the LNA improves when the radiation resistance of the antenna increases; the LNA used in this paper needs a minimum input resistance greater than about 0.2 Ω (varies depending on LNAs) at 20 MHz to operate adequately. Thus, we selected Sample A (in Fig. 2) that exhibits the maximum average gain

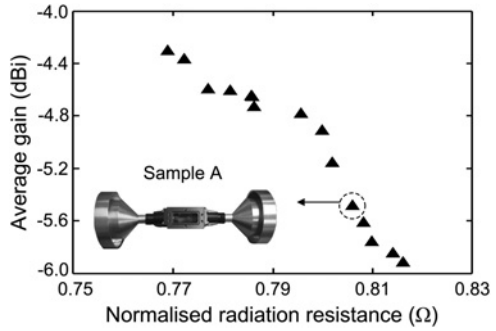

Figure 2 *Optimised results for the proposed antenna*

and, at the same time, satisfies the LNA's minimum requirement for input resistance. We then built and measured the performance of Sample A to confirm the optimised result. The optimised design parameters for Sample A were as follows: $w = 99.6$ mm, $r_1 = 80.4$ mm, $r_2 = 71.4$ mm, $r_3 = 74$ mm, $h_1 = 19.8$ mm, $h_2 = 176.2$ mm, $h_3 = 29.2$ mm, $h_4 = 25.4$ mm and $h_5 = 7.2$ mm. The antenna body, the multiconical sleeve and the skirt-shaped disk were made of aluminium, and the three parts were bolted together. An LNA was placed on the feed of the antenna to amplify the weak received signal, and that was shielded with a plastic case to protect the inner circuitry.

3 Measurement and analysis of the optimised DF antenna

3.1 Measurement in the low-frequency band (20–200 MHz)

The transmission loss (TL) is generally measured in an open site to profile the low-frequency (under about 200 MHz) radiation characteristics of the antenna under test (AUT) instead of measuring the antenna gain in an anechoic chamber. Fig. 3 shows the measured TL of the proposed antenna as a function of distance between the AUT and a transmitter. An LNA with a gain of about 15 dB is installed on the AUT, and a half-wavelength dipole [25] with an input power of 1 W is used as a transmitting antenna. The lengths of the dipoles are set to 3, 1.5 and 1 m at 50, 100 and 150 MHz, respectively. Both the AUT and transmitting antenna are raised above the surface of the ground by 1 m. The TL in Fig. 3 is then obtained by subtracting the LNA gain from the measurement to obtain the antenna performance without the effect of the LNA. Close agreement exists between the simulated and measured results of the proposed antenna. The slight difference between the simulation and measurement may have occurred because real environmental data such as the exact dielectric properties, shape of the ground soil and surrounding buildings were not included in our simulation. For the sake of comparison, the measured TL of the 60-cm conventional dipole is also plotted on the same graphs. The TL of the proposed antenna is almost the same as that of the 60-cm dipole even though the height of the antenna is reduced to 30 cm. As expected, the TL of each antenna increases as the frequency rises since the radiation resistances of the antennas also increase.

3.2 Measurement in the high-frequency band (200–1300 MHz)

We measured the passive part of the antenna without the LNA in an anechoic chamber for the frequency range 200–1300 MHz to estimate the performance of the AUT excluding the active circuit. The passive part of the proposed antenna was differentially fed with a 50-Ω characteristic impedance. To obtain the exact impedance from the differential feed antenna, we used a network

doi: 10.1049/iet-map.2008.0444

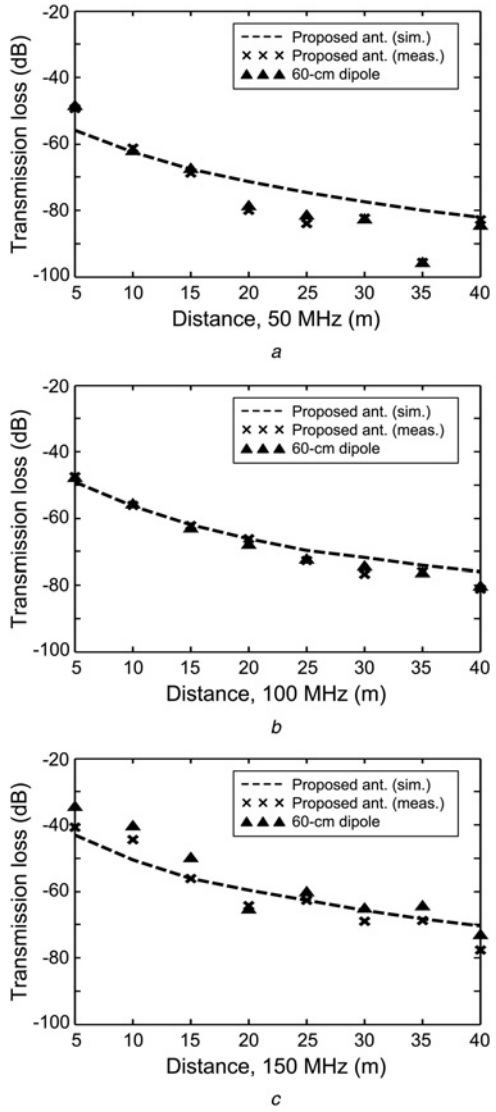

Figure 3 *TL of the proposed DF antenna and the 60-cm dipole*

a 50 MHz
b 100 MHz
c 150 MHz

analyser (Agilent E5071) that supports the measurement of balanced ports. We also constructed and used an impedance transformer that converts two single-ended 50-Ω ports connected to the network analyser to a 50-Ω differential port connected to the antenna. The inset in Fig. 4 shows the impedance transformer printed on an FR-4 substrate ($\varepsilon_r = 4.3$, $\tan\delta = 0.02$, thickness = 1.6 mm) with a 21 × 20-mm ground plate. The solid and dashed lines in Fig. 4 represent the measured and simulated return losses of the proposed DF antenna using the impedance transformer we constructed. The measurement closely matches the simulation result except in the range 300–500 MHz because of the power loss of the impedance transformer. Again, the return loss of the 60-cm dipole is plotted in the same figure. The proposed antenna resonates at 200 MHz as does the 60-cm dipole antenna, although

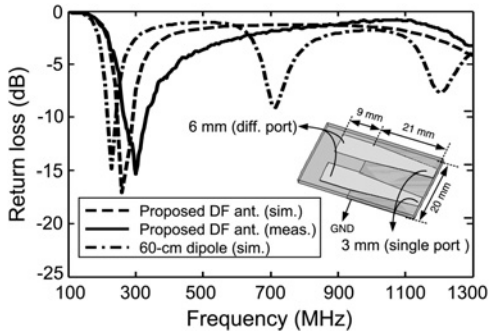

Figure 4 *Return loss of the proposed antenna and the 60-cm dipole*

the proposed antenna is only half the size. As expected, the harmonic resonance of the proposed antenna shifts to a much higher frequency than 1300 MHz because of the disk loading effect, unlike the 60-cm dipole. Note that the 60-cm dipole exhibits the harmonic resonance (current distribution on around 1.5λ) between 700 and 900 MHz. We would expect from this result that the radiation null of the proposed antenna would be eliminated in the operating frequency band.

The realised gain of the proposed DF antenna in the broadside direction ($\theta = 90^\circ$) was measured as shown in Fig. 5 using two identical antennas with the constructed impedance transformer. The measured gain was close to the simulated result, and the proposed antenna had a stable gain without large fluctuating values across a wide frequency band. However, as expected, the 60-cm dipole showed a radiation null at about 850 MHz since the currents on the antenna are distributed at about 2λ, and they almost cancel in the far-field region. In the operating band, the proposed antenna showed a broad simulated beamwidth (for the DF antenna, this is defined as a gain greater than −15 dBi) of more than 100°. We also measured the radiation efficiency (which excludes the mismatch loss at the input port) of the antenna using the Wheeler cap. This was greater than 95% in the operating frequency band [26, 27].

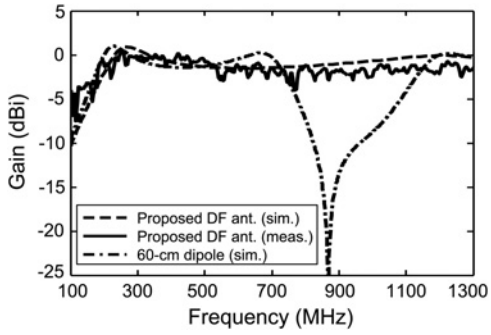

Figure 5 *Broadside gain of the proposed DF antenna and the 60-cm dipole*

Fig. 6 shows a comparison of the measured radiation patterns of the proposed antenna and the 60-cm dipole. The radiation pattern of the proposed antenna remains omnidirectional without any nulls in the broadside direction up to a frequency of 1300 MHz, whereas the 60-cm dipole shows a gain that is drastically reduced in the broadside direction at 800 MHz, with a large fluctuation in the *E*-plane at 1200 MHz.

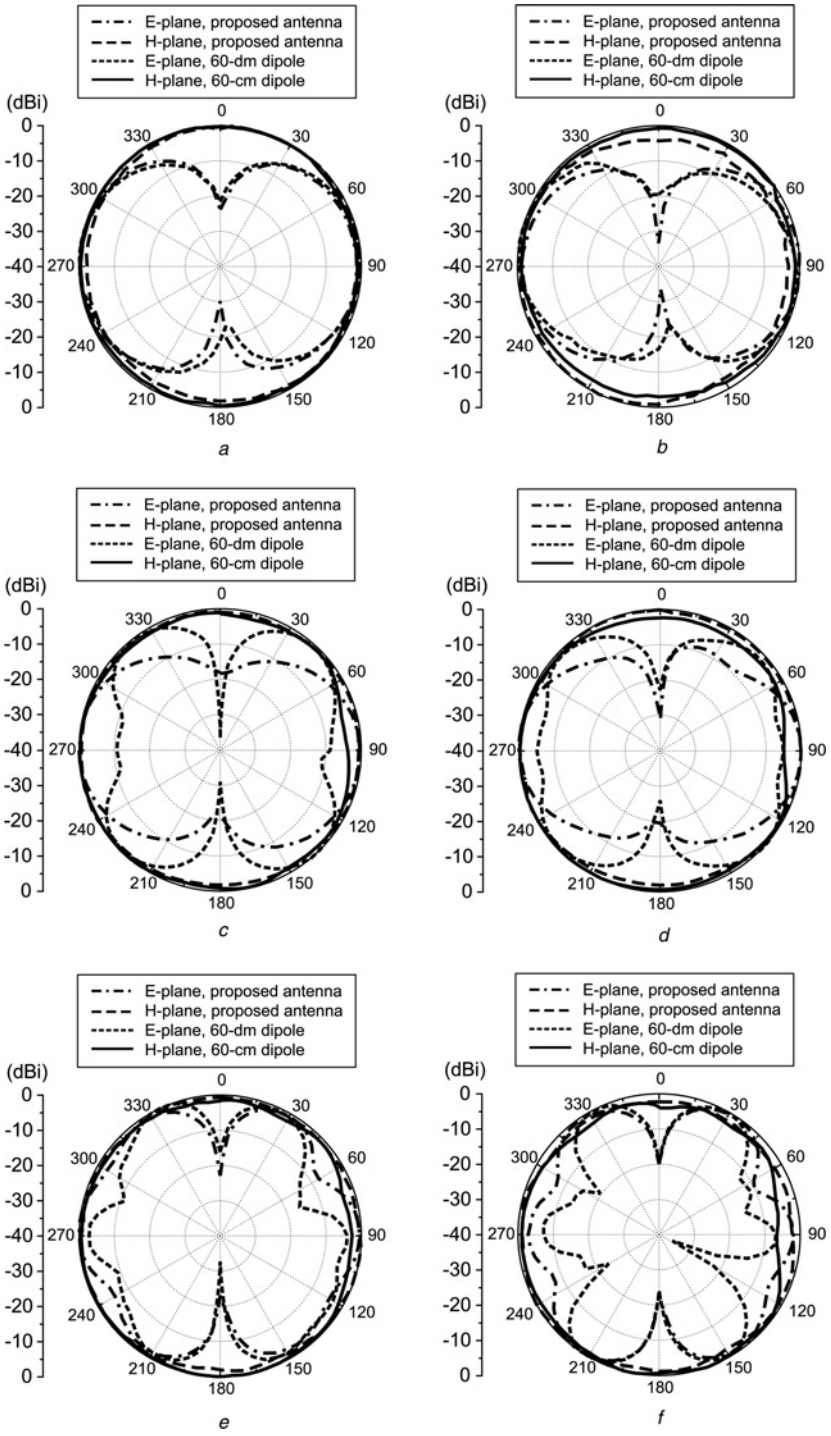

Figure 6 *Measured radiation pattern of the proposed DF antenna and the 60-cm dipole*

a 200 MHz
b 500 MHz
c 800 MHz
d 900 MHz
e 1100 MHz
f 1200 MHz
Dashed-dotted line: *E*-plane, proposed antenna; dashed line: *H*-plane, proposed antenna; dotted line: *E*-plane, 60-cm dipole and solid line: *H*-plane, 60-cm dipole

IET Microw. Antennas Propag., 2010, Vol. 4, Iss. 7, pp. 930–937

doi: 10.1049/iet-map.2008.0444

3.3 Operating principle of the DF antenna

To explain the operating principle of the proposed antenna, we examined how the loaded disk affects the radiation pattern, and how the multiconical sleeve boosts the input resistance of the antenna. First, to understand the effect of the loaded disk, we plotted the broadside gain for various disk sizes as shown in Fig. 7*a*. Two different sizes of disk-loaded antennas were built with the heights of 28 and 40 cm to maintain the same resonance frequency at 200 MHz. Fig. 7*a* clearly shows that the radiation null shifts to a much higher frequency as the size of the loaded disk increases. Fig. 7*b* shows the current distributions on each antenna body at 850 MHz. In the 60-cm dipole, the currents with different signs are distributed over 2λ, and the radiation from the opposite currents cancels out in the broadside direction. However, in the antenna with the disk loading, the induced currents on the antenna body are distributed over less than 2 λ, and as a result, nulls in the broadside direction do not occur over a wide frequency band. Fig. 8 shows the null frequencies in the broadside direction for various disk sizes obtained using the FEKO EM simulator. All antennas were built to resonate at 200 MHz. As the disk size increases, the null frequency increases because the current distribution of the antenna body becomes shorter. This result clearly shows that the electrical size of the disk significantly affects the frequency where the radiation null occurs.

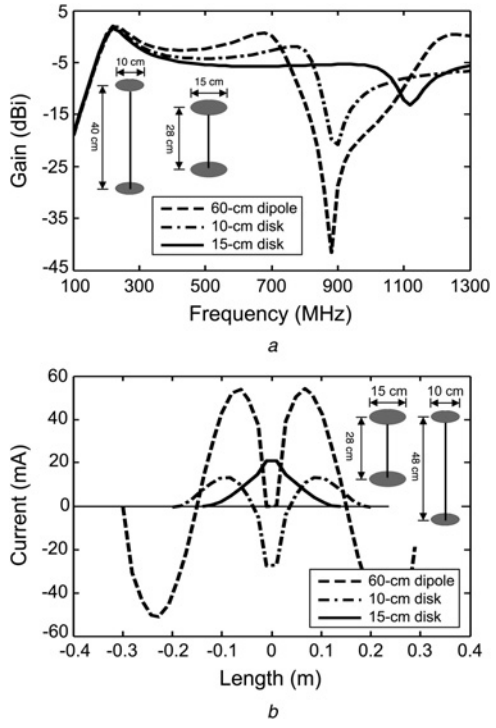

Figure 7 *Effect of the loaded disk*

a Simulated broadside gain for various loaded disk sizes
b Simulated current distribution at 850 MHz for various loaded disk sizes

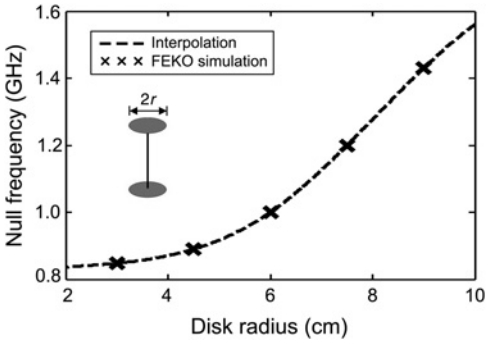

Figure 8 *Null frequency as a function of loaded disk size (radius = 8 mm)*

To examine the effect of the multiconical sleeve, we compared the input resistance and the realised gain among an antenna with a conical sleeve ($a = 50$ mm, $b = 70$ mm; parameters shown in the inset in Fig. 9), a thick dipole with a radius of 8 mm, and a thin dipole of aluminium pipe with a radius of 0.4 mm. Dipoles with a thick radius are usually used to increase the input resistance in the design of electrically small antennas. However, Fig. 9 shows that the conical sleeve more effectively increases the input resistance and the realised gain than the thick radius of the dipole. This effect occurs because the total path and the surface area for the current flow are increased by adding the multiconical sleeve, and thus it raises the input resistance while preserving the physical height of the antenna. Fig. 10 shows the input resistance as a function of the total surface length $(4d_1 + d_2)$ of the conical sleeve, which is simplified to two sections without the loaded disk. The height of the antenna is fixed at 30 cm (0.02λ), and then the surface length of the conical sleeve is changed by increasing the angle α and the length d_1. The highest input resistances of each antenna ($\alpha = 30^\circ$, 40° and 50°) are marked with a solid triangle, and they occur when the length of the conical sleeve $(2d_1)$ is similar to the length of the antenna body (d_2) for a given angle. This result demonstrates that high-input resistance can be achieved if the angle and surface length of the conical sleeve are properly selected although the total height of the antenna does not change.

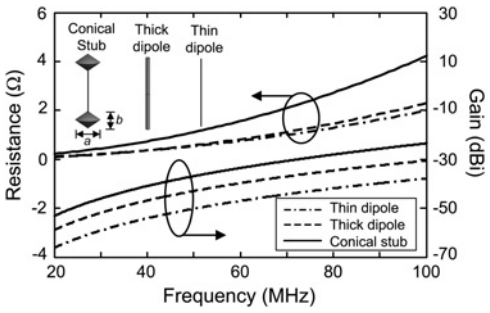

Figure 9 *Input resistances and gains of a thin dipole, thick dipole and conical sleeve loaded antenna*

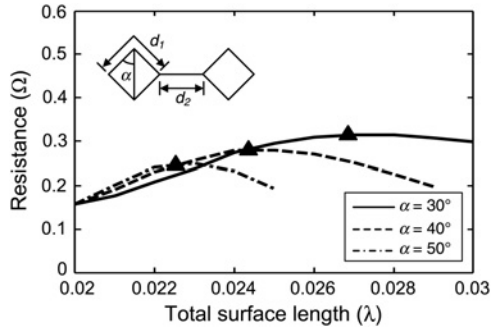

Figure 10 *Input resistance for various sizes of conical sleeve (radius = 0.4 mm)*

4 Conclusions

We proposed a novel electrically small antenna for a mobile DF system. In the low-frequency band (20–200 MHz), the proposed antenna exhibits an increased input resistance because of the multiconical sleeve, and shows a receiving performance similar to the conventional 60-cm dipole while the height of antenna is reduced to 30 cm. In the high-frequency band (200–1300 MHz), the proposed antenna maintains an omnidirectional radiation pattern with a stable realised gain because of the skirt-shaped disk, whereas the 60-cm dipole has a radiation null in the broadside direction at about 850 MHz. To explain the operating principle of the proposed antenna, we described how the loaded disk shifts the broadside null and the conical sleeve boosts the input resistance.

5 Acknowledgments

This study was supported by the IT R&D program of MKE/IITA (2009-F-042-01, A Study on Mobile Communication System for Next-Generation Vehicles with Internal Antenna Array).

6 References

[1] LE-NGOC S., LE-NGOC T.: 'Precision direction finding antennas', *IEEE Trans. Consum. Electron.*, 1990, **36**, (4), pp. 918–921

[2] PRESTON S.L., THIEL D.V., SMITH T.A., O'KEEFE S.G., LU J.W.: 'Base-station tracking in mobile communications using a switched parasitic antenna array', *IEEE Trans. Antennas Propag.*, 1998, **46**, (6), pp. 841–844

[3] CHARPENTIER E., LAURIN J.-J.: 'An implementation of a direction-finding antenna for mobile communications using a neural network', *IEEE Trans. Antennas Propag.*, 1999, **47**, (7), pp. 1152–1159

[4] LIANG X., CHIA Y.W.M.: 'New precision wideband direction finding antenna', *IEE Proc. Microw. Antennas Propag.*, 2001, **148**, (6), pp. 363–364

[5] KALIS A., ANTONAKOPOULOS T.: 'Direction finding in IEEE 802.11 wireless networks', *IEEE Trans. Instrum. Meas.*, 2002, **51**, (5), pp. 940–948

[6] CHOI J.-H., SO J.-H., PARK C.-S., OH S.-S.: 'Active composite dipole antenna for direction finding array antenna application'. IEEE Antennas Propag. Soc. Symp., 2006, pp. 1153–1156

[7] TAKAYAMA T., SATO M.: 'A novel direction-finding algorithm for directional borehole radar', *IEEE Trans. Geosci. Remote Sens.*, 2007, **45**, (8), pp. 2520–2528

[8] STUTZMAN W.L., THIELE G.A.: 'Antenna theory and design' (Wiley, New York, 1998, 2nd edn.)

[9] Electromagnetic Waves and Antennas: http://www.ece.rutgers.edu/~orfanidi/ewa

[10] BALANIS C.A.: 'Antenna theory: analysis and design' (Wiley, New York, 1997, 2nd edn.)

[11] BENNETT W.S.: 'A basic theorem that simplifies the analysis of wire antennas', *IEEE Antennas Propag. Mag.*, 1998, **40**, (1), pp. 22–30

[12] ADD195 http://www.rsd.de/www/dev_center.nsf/html/ddf195misc

[13] JUNG C.W., KIM Y.J., KIM Y.E., DE FLAVIIS F.: 'Macro-micro frequency tuning antenna for reconfigurable wireless communication systems', *Electron. Lett.*, 2007, **43**, (4), pp. 201–202

[14] MUELLER R., LORCH R., SCHOPP R., MENZEL W.: 'A HF/VHF direction finding antenna with optimized radar cross section'. IEEE Antennas Propag. Soc. Symp., 2007, pp. 1153–1156

[15] Chapter 3 classical DF methods: http://www.rohde-schwarz.com/www/downcent.nsf/file/chapter3_classical_df_methods.pdf

[16] JOHNSON D.H., DUDGEON D.E.: 'Array signal processing: concepts and techniques' (Prentice-Hall, Englewood Cliffs, NJ, 1993)

[17] FEKO: http://www.feko.info

[18] GOLDBERG D.: 'Genetic algorithms in search, optimization and machine learning' (Addison Wesley, Boston, 1989)

[19] RAHMAT-SAMII Y., MICHIELSSEN E.: 'Electromagnetic optimization by genetic algorithms' (Wiley, New York, 1999)

doi: 10.1049/iet-map.2008.0444

[20] HAUPT R.L., WERNER D.H.: 'Genetic algorithms in electromagnetics' (Wiley, New York, 2007)

[21] SRINIVAS N., DEB K.: 'Multiobjective optimization using nondominated sorting in genetic algorithms', *J. Evol. Comput.*, 1995, **2**, (3), pp. 221–248

[22] HORN J., NAFPLIOTIS N., GOLDBERG D.E.: 'A niched Pareto genetic algorithm for multiobjective optimization'. Proc. First IEEE Conf. on Evolutionary Computation, June 1994, pp. 82–87

[23] WEILE D.S., MICHIELSSEN E.: 'Genetic algorithm optimization applied to electromagnetics: a review', *IEEE Trans. Antennas Propag.*, 1997, **45**, (3), pp. 343–353

[24] HOORFAR A.: 'Evolutionary programming in electromagnetic optimization: a review', *IEEE Trans. Antennas Propag.*, 2007, **55**, (3), pp. 523–537

[25] Adjustable dipole: http://www.ets-lindgren.com/manuals/3121C.pdf

[26] NEWMAN E., BOHLEY P., WALTER C.: 'Two methods for the measurement of antenna efficiency', *IEEE Trans. Antennas Propag.*, 1975, **23**, (4), pp. 457–461

[27] CHOO H., ROGERS R., LING H.: 'On the Wheeler cap measurement of the efficiency of microstrip antennas', *IEEE Trans. Antennas Propag.*, 2005, **53**, (7), pp. 2328–2332